*ORIGINAL ARTICLE*

Annals of Agricultural and Environmental Medicine
www.aaem.pl

# The mechanism of Scleromitrion diffusum (Willd.) R. J. Wang ethanol extract combined with carboplatin in treating cervical cancer

**Mengying Gao**[1,A-C,E-F] ✉, **Chenying Su**[2,A-D,F], **Dulin Zhang**[2,A-D,F]

[1] *Department of Gynaecology, Fujian Provincial People's Hospital, Fujian, China*
[2] *Fujian University of Traditional Chinese Medicine, Fujian, China*
*A – Research concept and design, B – Collection and/or assembly of data, C – Data analysis and interpretation, D – Writing the article, E – Critical revision of the article, F – Final approval of the article*

Gao M, Su C, Zhang D. The mechanism of Scleromitrion diffusum (Willd.) R. J. Wang ethanol extract combined with carboplatin in treating cervical cancer. Ann Agric Environ Med. doi:10.26444/aaem/240303

## Abstract

**Introduction and Objective.** Cervical cancer (CC) is a common cancer in women worldwide, imposing a substantial burden on healthcare systems. The aim of the study is to evaluate the effects of Scleromitrion diffusum (Willd.) R.J.Wang (SD) in combination with carboplatin (CBP) on CC cells, and to elucidate the underlying molecular mechanisms.

**Materials and Method**. The half-maximal inhibitory concentration ($IC_{50}$) of SD and CBP in HeLa and CaSki cells was determined using the cell counting kit-8 (CCK-8) assay. Cell migration and invasion were assessed by Transwell assays. Levels of interleukin-6 (IL-6), tumour necrosis factor-alpha (TNF-α), and intracellular reactive oxygen species (ROS) were measured using enzyme-linked immunosorbent assay (ELISA). The expression of arachidonate 5-lipoxygenase (ALOX5) was analyzed via reverse transcription-quantitative polymerase chain reaction (RT-qPCR). In addition, the effects of combined SD and CBP treatment, as well as ALOX5 knockdown, on the malignant behaviour of cancer cells were investigated.

**Results.** The results obtained demonstrated that SD effectively inhibited the proliferation, migration, and invasion of HeLa and CaSki cells. The combination of SD and CBP exhibited a synergistic effect, leading to further suppression of these malignant phenotypes. Mechanistically, the combined treatment elevated the levels of IL-6, TNF-α, and ROS, and down-regulated ALOX5 expression. Notably, knockdown of ALOX5 expression was shown to suppress the malignant behaviours of both HeLa and CaSki cells.

**Conclusions**. The combined application of SD and CBP markedly suppressed malignant phenotypes in HeLa and CaSki cells.

## Key words

cervical cancer, carboplatin, ALOX5, scleromitrion diffusum (Willd.) R.J.Wang

## INTRODUCTION AND OBJECTIVE

Based on the International Federation of Gynaecology and Obstetrics (FIGO) 2009 staging criteria, the standard treatment for locally advanced cervical cancer (CC, stages IB2–IVA) is platinum-based concurrent chemoradiotherapy [1]. Platinum compounds, notably cisplatin and carboplatin (CBP), exert their anticancer effects primarily by interfering with nucleotide metabolic pathways, but their efficacy in CC is limited by tumour evolution and tissue heterogeneity, which contribute to significant side-effects and the development of drug resistance [2]. Given these limitations, there is an urgent need for novel therapies that are both safer and more effective against CC.

*Scleromitrion diffusum* (Willd.) R.J.Wang (SD), also known as Hedyotis diffusa, is a medicinal plant with neuroprotective, anti-inflammatory, and antioxidant properties. Previous studies have shown that the ethanol extract of SD is rich in flavonoids and exhibits potential anticancer activity. For example, this extract has been shown to inhibit the viability of HepG2.2.15 and Hep3B hepatocellular carcinoma cells *in vitro* [3]. Additionally, studies have reported that the two main flavonoid components in SD – quercetin and kaempferol – play a significant role in CC. Quercetin not only inhibits proliferation and induces apoptosis in CC cells [4, 5] but also suppresses cell migration and invasion, thereby attenuating the malignant behaviours of CC cells [6]. Moreover, quercetin may help reverse cisplatin resistance in CC [7]. Kaempferol also shows promising anti-CC activity by inducing apoptosis and autophagy [8]. It has been shown to down-regulate key glycolytic enzymes via multiple signalling pathways, including PI3K/AKT/HIF-1α and JAK2/STAT3, thus inhibiting CC progression [9]. Furthermore, Kaempferol can also induce apoptosis in CC cells and inhibit inflammation by regulating inflammatory cytokines and enhancing antioxidant defense [10].

Importantly, the anti-cancer activities of quercetin and kaempferol are closely linked to their regulatory effects on arachidonic acid metabolism, particularly through the modulation of arachidonate lipoxygenases (ALOXs). Quercetin inhibits the expression of arachidonate lipoxygenase 5 (ALOX5), thereby suppressing apoptosis, inflammation, and ferroptosis in LPS-induced AC16 cells [12]. Similarly, kaempferol has been shown to inhibit lipoxygenase activity, thereby interfering with the formation of pro-inflammatory leukotrienes and hepoxilins [14]. By targetting the arachidonic acid metabolic pathway at the lipoxygenase level, these flavonoids reduce the production of lipid mediators that promote tumour cell proliferation, survival, and metastasis [15]. This mechanism provides

✉ Address for correspondence: Mengying Gao, Department of Gynaecology, Fujian Provincial People's Hospital, Fuzhou, China
E-mail: FZGaomengying@163.com

Received: 13.01.2026; accepted: 24.09.2026; first published:

a molecular basis for understanding how quercetin and kaempferol exert their anti-cancer effects in CC, and establishes a critical connection between the bioactive components of SD and ALOX-mediated carcinogenesis.

ALOXs are key enzymes that catalyze the conversion of polyunsaturated fatty acids into lipid hydroperoxides, which contribute to cell membrane damage and ferroptosis [16]. Among them, ALOX5 functions as a dioxygenase and plays a central role in regulating inflammation. It is also closely linked to the progression of various cancers. ALOX5 contributes significantly to CC pathogenesis. An $ALOX5^+$ tumour-associated macrophage subset with notable pro-tumour transformation capacity has been identified in CC tissues and may influence disease progression [17]. Depletion of ALOX5 has been shown to inhibit cell growth by approximately 70% and induce apoptosis in roughly 50% of CC cells [18]. Additionally, in the HeLa cell line, altered ALOX5 expression promotes ferroptosis, thereby further affecting the biological behaviour of CC cells [19].

Based on the aforementioned background, this study was designed to evaluate the anti-CC activity of the SD ethanol extract and to elucidate the mechanism underlying the combined therapeutic effect of SD with CBP (SD+CBP), providing a novel therapeutic strategy for CC treatment.

## MATERIALS AND METHOD

**Preparation of SD extract.** SD was purchased from Shanghai Yuanye Bio-Technology (S27202). SD herb material was supplied as dried whole-plant powder and authenticated by the pharmaceutical department according to the Pharmacopoeia of the People's Republic of China (2020 edition) specifications. The powder was subjected to triplicate reflux extraction (100 °C, 2 hours per cycle) in 10 volumes of 70% ethanol. Following filtration and concentration, the extract was lyophilized and stored at 4 °C. The SD extract was prepared and purified following a previously reported protocol, and its main flavonoid components were identified as quercetin, kaempferol, and scutellarein [20]. To ensure batch-to-batch consistency, raw materials were obtained from the same source, all extractions were performed in parallel, and three 3 independent preparations were carried out.

**Cell culture and treatment.** This study used the CC cell lines HeLa (Sitaimo, STM-CL-5112) and CaSki (Shang En Biotechnology, SNL-067), as well as the normal human cervical epithelial cell line HUCEC (Yaji Biological, YS1079C). HeLa cells were maintained in DMEM medium (Thermo Fisher, 12491015) supplemented with 10% foetal bovine serum (FBS) (Sigma-Aldrich, F0193), 100 U/mL penicillin (P0389), and 100 µg/mL streptomycin (S9137). HUCEC and CaSki cells were cultured in RPMI-1640 medium (R8758). CBP (C2538, 100 mg, purity ≥ 99%) was employed as the chemotherapeutic agent.

**Measurement of cytotoxic synergy.** Drug synergy was evaluated using the Chou–Talalay median-effect method [21], implemented in CalcuSyn software (Biosoft, Version 2.1). The combination index (CI) was calculated to quantify drug interactions, with CI = 1 indicating additivity, CI > 1 antagonism, and CI < 1 synergy.

**Identification of potential therapeutic targets.** Potential target genes associated with CC were identified through the GeneCards database (www.genecards.org), while putative targets of SD were retrieved from the TCMSP database (www.tcmsp-e.com).

**ALOX5 transfection assay.** Transfection was performed using Lipofectamine 2000 liposomal transfection reagent (Thermo Fisher, 11668030). The following constructs were transfected: ALOX5 knockdown plasmid (si-ALOX5), empty vector plasmid (si-NC). Transfection efficiency was assessed by quantitative polymerase chain reaction (qPCR) analysis of ALOX5 mRNA levels 48 hours post-transfection.

**Reverse transcription-quantitative polymerase chain reaction (RT-qPCR).** Total RNA extraction was performed with a commercial RNA/Protein Isolation Kit (Beyotime, R0018S). Following extraction, 1 µg of total RNA underwent reverse transcription in a 20 µL reaction system using PrimeScript™ RT Master Mix (Takara, RR036Q). The resulting cDNA was stored at -20 °C until further use. qPCR reactions were prepared with SYBR Premix Ex Taq™ (Takara, RR390Q) in a total volume of 20 µL, employing cDNA as the template. Relative gene expression was quantified via the $2^{-\Delta\Delta Ct}$ method, with GAPDH serving as the internal control. Each sample was tested in 3 independent biological replicates (n=3) and 3 technical replicates.

**Enzyme-linked immunosorbent assay (ELISA).** Levels of interleukin-6 (IL-6) and tumor necrosis factor-alpha (TNF-α) were quantified using commercially available human ELISA kits (IL-6: Beyotime, PI330; TNF-α: PT518). Intracellular reactive oxygen species (ROS) levels were measured with a human ROS ELISA kit (Gilead Sciences, J21799), a kit that uses a double-antibody sandwich method to detect ROS content. Purified anti-ROS capture antibodies were pre-coated onto microplates; ROS in samples were captured and further bound with horseradish peroxidase (HRP)-conjugated detection antibodies to form immune complexes. Briefly, samples were incubated in pre-coated wells with a specific capture antibody, followed by the addition of an HRP-conjugated detection antibody. After washing, colour development was initiated by adding 3,3′,5,5′-tetramethylbenzidine (TMB) substrate. Absorbance was then measured at a wavelength of 450 nm. Each ELISA detection was performed in 3 independent biological replicates (n=3).

**Cell counting kit-8 (CCK-8) assay.** The CCK-8 (Beyotime, C0037) was used to assess cell viability. After treatment with a series of drug concentrations (including controls) for 24, 48, or 72 hours, 10 µL of CCK-8 solution was added to each well and gently mixed. After a specified incubation period, the optical density (OD) at 450 nm was measured for all wells simultaneously using a microplate reader (Detiebio). Each concentration group was set with 3 independent replicates (n=3), and each replicate contained 3 technical repeats. The inhibition rate (IR) was derived using the standard formula:

$$IR = \frac{OD\ control - OD\ treated}{OD\ control} \times 100\%$$

**Transwell assay.** Cell migration and invasion were assessed with Transwell chambers (8.0 µm pore size; Corning, 3422).

For the invasion assay, the chamber membranes were pre-coated with Matrigel (BD Biosciences, 354230). In both assays, cell suspensions were placed in the upper chamber, and the lower chamber was filled with DMEM containing 10% FBS as a chemo-attractant. Migration assays were performed using uncoated membranes. After incubation, cells that had traversed the membrane were fixed and stained. Images were captured under an optical microscope (PRECISE), and the number of migrated or invaded cells per field was quantified. Each group was tested in 3 independent replicates (n=3), and 5 random fields were counted per replicate.

**Statistical analysis.** Results are expressed as mean ± standard deviation from at least 3 independent replicates. All statistical analyses were conducted with GraphPad Prism 9.3.1 software. Inter-group comparisons were performed using Student's t-test for 2 groups, while two-way analysis of variance (ANOVA) was applied to datasets involving 2 independent factors. A *p*-value below 0.05 was considered statistically significant.

## RESULTS

**Effects of SD on HeLa and CaSki cell function.** To determine the effect of SD on the proliferation of HeLa and CaSki cells, a dose-response experiment was conducted over 24, 48, and 72 hours. The data indicated that SD inhibited the proliferation of both cell lines in a concentration-dependent manner (Fig. 1A-B). The half-maximal inhibitory concentrations ($IC_{50}$) of SD were determined in both cell lines. In HeLa cells, the $IC_{50}$ values were 117.10 µmol/L (95% confidence interval [CI]: 104.30–133.20) at 24 h, 36.51 µmol/L (95% CI: 31.24–42.71) at 48 h, and 21.70 µmol/L (95% CI: 19.66–24.33) at 72 h. In CaSki cells, the corresponding $IC_{50}$ values were 160.00 µmol/L (95% CI: 131.70–203.80) at 24 h, 50.08 µmol/L (95% CI: 42.67–58.95) at 48 h, and 27.03 µmol/L (95% CI: 22.78–32.28) at 72 h. The 48-h $IC_{50}$ value was subsequently selected for further experiments. Transwell assays demonstrated that SD notably inhibited the migratory and invasive capacities of both cell lines (Fig. 1C-D).

**CI analysis of SD combined with CBP.** Using the Chou-Talalay method, the synergistic effect of SD combined with CBP was evaluated in HeLa and CaSki cells. After 48-hour treatment, CBP alone exhibited dose-dependent inhibition in both cell lines. The $IC_{50}$ of CBP was 136.4 µmol/L (95% CI: 126.4–147.3) in HeLa cells (Fig. 2A) and 250.6 µmol/L (95% CI: 200.3–330.6) in CaSki cells (Fig. 2B). Median-effect analysis (Fig. 2C-2D) for single agents and the combination revealed linear correlations ($r > 0.95$). Fig. 2E and F show the dose-effect curves of SD, CBP alone, and the combination of SD + CBP in 2 cell lines. The results demonstrated that the combination curve was markedly left-shifted relative to single-agent treatments, indicating stronger growth inhibitory efficacy of the combined treatment. Fa-CI plot analysis (Fig. 2G-H) shows that at ED50, the CI values were 0.652 for HeLa cells and 0.632 for CaSki cells. Both values were below 0.7, indicating a synergistic effect. In conclusion, a synergistic anti-proliferative effect of SD and CBP was observed in both HeLa and CaSki cell lines.

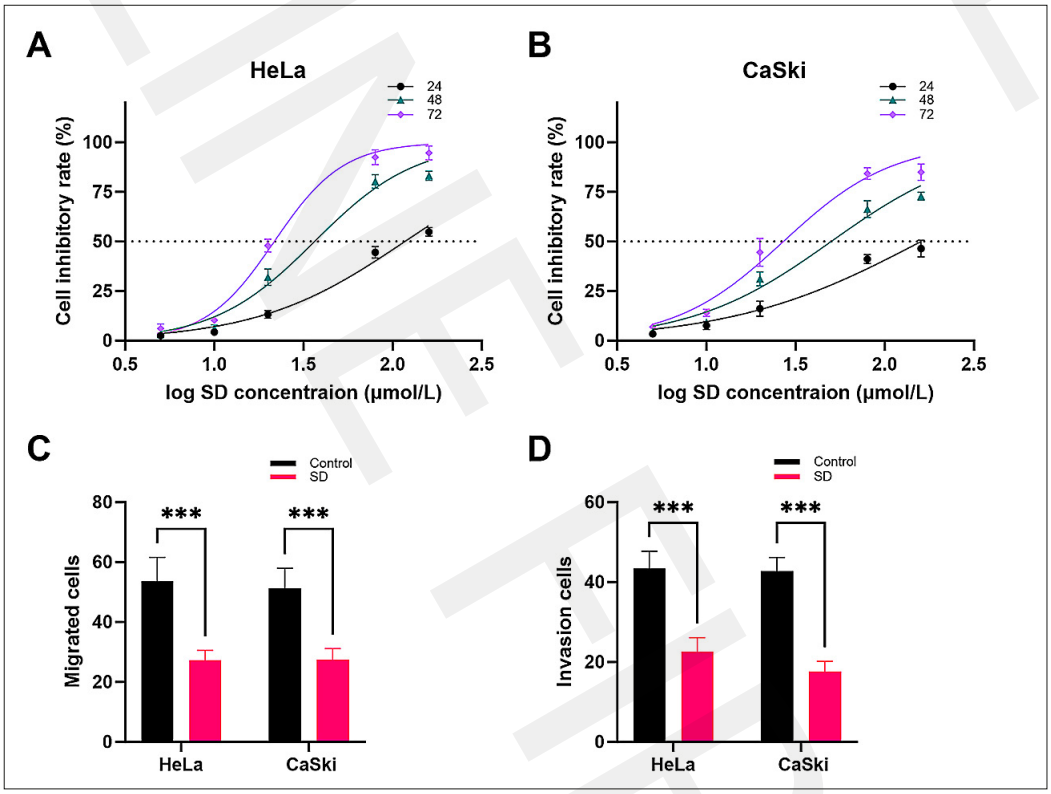



**Figure 1.** Effects of SD on proliferation, migration, and invasion in HeLa and CaSki cells. **(A)** Viability of HeLa cells following treatment with different concentrations of SD at 24, 48, and 72. **(B)** Viability of CaSki cells following treatment with different concentrations of SD at 24, 48, and 72 h. **(C)** Migration abilities of HeLa and CaSki cells after treatment with SD for 48 h. **(D)** Invasion abilities of HeLa and CaSki cells after treatment with SD for 48 h. Data are presented as mean ± SD from 3 independent experiments (n=3).
***$p < 0.001$

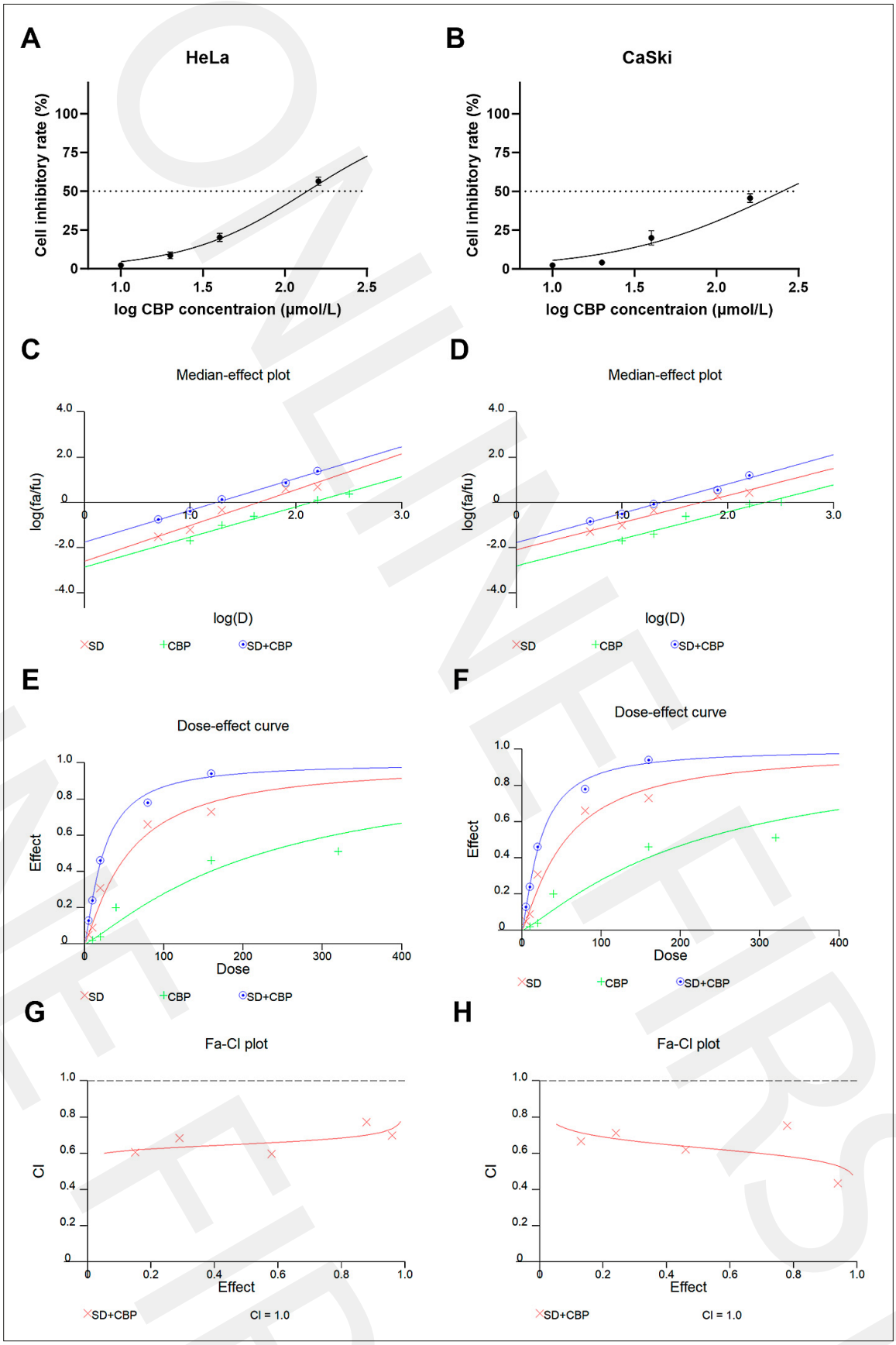



**Figure 2.** Evaluation of the synergistic interaction between SD and CBP. (**A**) Viability of HeLa cells treated with increasing concentrations of CBP for 48 h. (**B**) Viability of CaSki cells treated with increasing concentrations of CBP for 48 h. **(C)** Median-effect analysis of SD and CBP combination treatment in HeLa cells. (**D**) Median-effect analysis of SD and CBP combination treatment in CaSki cells. (**E**) Dose-response curves of SD, CBP alone, and their combination in HeLa cells. (**F**) Dose-response curves of SD, CBP alone, and their combination in CaSki cells. (**G**) Fa-CI plot for CBP and SD combination in HeLa cells. (**H**) Fa-CI plot for CBP and SD combination in CaSki cells. Data were obtained from 3 independent experiments (n=3)

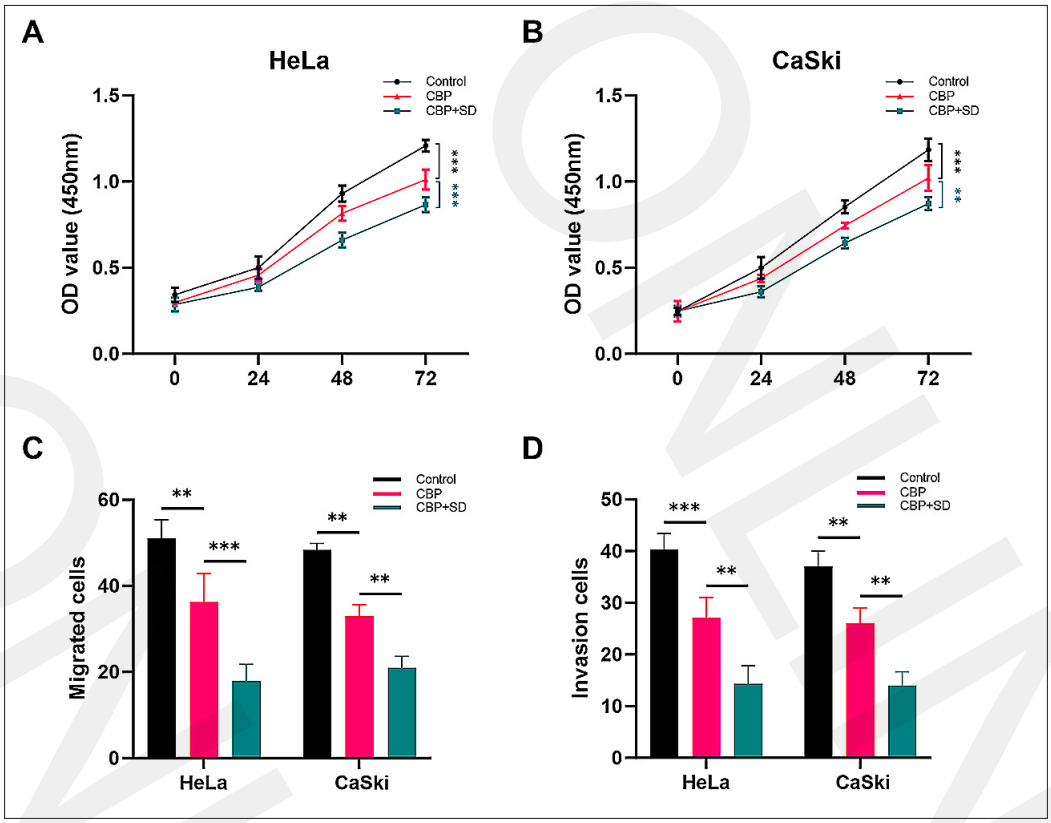



**Figure 3.** Effects of SD combined with CBP on biological functions of HeLa and CaSki cells. **(A)** Viability of HeLa cells after treatment with SD, CBP alone, or their combination. (**B**) Viability of CaSki cells after treatment with SD, CBP alone, or their combination. (**C**) Migration abilities of HeLa and CaSki cells under SD and CBP combined treatment. (**D**) Invasion abilities of HeLa and CaSki cells under SD and CBP combined treatment. Data are expressed as mean ± SD of 3 independent experiments (n=3).
$^{**}p < 0.01$; $^{***}p < 0.001$

**Influence of SD combined with CBP on HeLa and CaSki cell function.** In this study, the IC50 concentrations of SD and CBP were chosen for combination experiments. IC50 levels were selected to ensure a moderate but consistent cytotoxic background, which allows for clear and reliable detection of synergistic growth inhibition. In contrast to sub-inhibitory concentrations such as IC25/IC30, which may produce weak and variable effects, IC50 values provide a sufficiently robust baseline to unambiguously distinguish enhanced efficacy of the combination from individual agent effects. As shown in Figure 3A-B, compared to control, treatment with CBP alone significantly reduced cell viability in both HeLa and CaSki cell lines. This inhibitory effect was substantially greater when CBP was combined with SD, suggesting an enhancement of the anti-proliferative activity. Furthermore, in Transwell migration and invasion assays, CBP monotherapy attenuated both processes. The combination of SD and CBP resulted in a more pronounced suppression of cell migration and invasion (Fig. 3C-D). Taken together, these functional assays demonstrated that, relative to CBP monotherapy, the combination of SD and CBP produces a more potent effect in suppressing proliferation and inhibiting the migratory and invasive capacities.

**Mechanistic exploration of the combination of SD and CBP.** To further explore the mechanisms underlying the combination therapy, its influence on inflammatory pathways and oxidative stress was assessed. Notably, previous studies have linked elevated levels of inflammatory cytokines, including IL-6 and TNF-α, to an increased risk of CC [22, 23]. Elevated levels of IL-6 and TNF-α were observed after single-agent treatment with CBP or SD (Fig. 4A-B). This induction was further augmented by combination treatment, indicating that the 2 agents act synergistically to strongly activate pro-inflammatory signaling. Oxidative stress is also involved in CC progression [24]. Detection results showed that both SD and CBP monotherapy significantly increased intracellular ROS levels. The increase in ROS levels was even more pronounced in the combined therapy group (Fig. 4C).

Furthermore, potential targets of SD and genes associated with CC were obtained by intersecting the TCMSP and GeneCards databases. Among the 5 overlapping targets identified, ALOX5 was selected for further mechanistic investigation (Fig. 4D) due to its high association score with CC in GeneCards (score: 61) and its documented role in regulating inflammatory and oxidative stress pathways [25], which aligns with the phenotypic observations of this study. Experimental results showed that SD significantly suppressed ALOX5 expression, and this inhibitory effect was more pronounced in the combination treatment group (Fig. 4E).

These findings suggested that SD and CBP may enhance their anti-CC effects by co-regulating the ALOX5-mediated inflammation-oxidative stress axis.

**Impact of ALOX5 expression on the biological behaviour of HeLa and CaSki cells.** Initial analysis of ALOX5 expression in HeLa and CaSki cells revealed significantly elevated mRNA levels compared to normal cervical epithelial cells (HUCEC). Subsequently, 48 hours post-transfection, knockdown

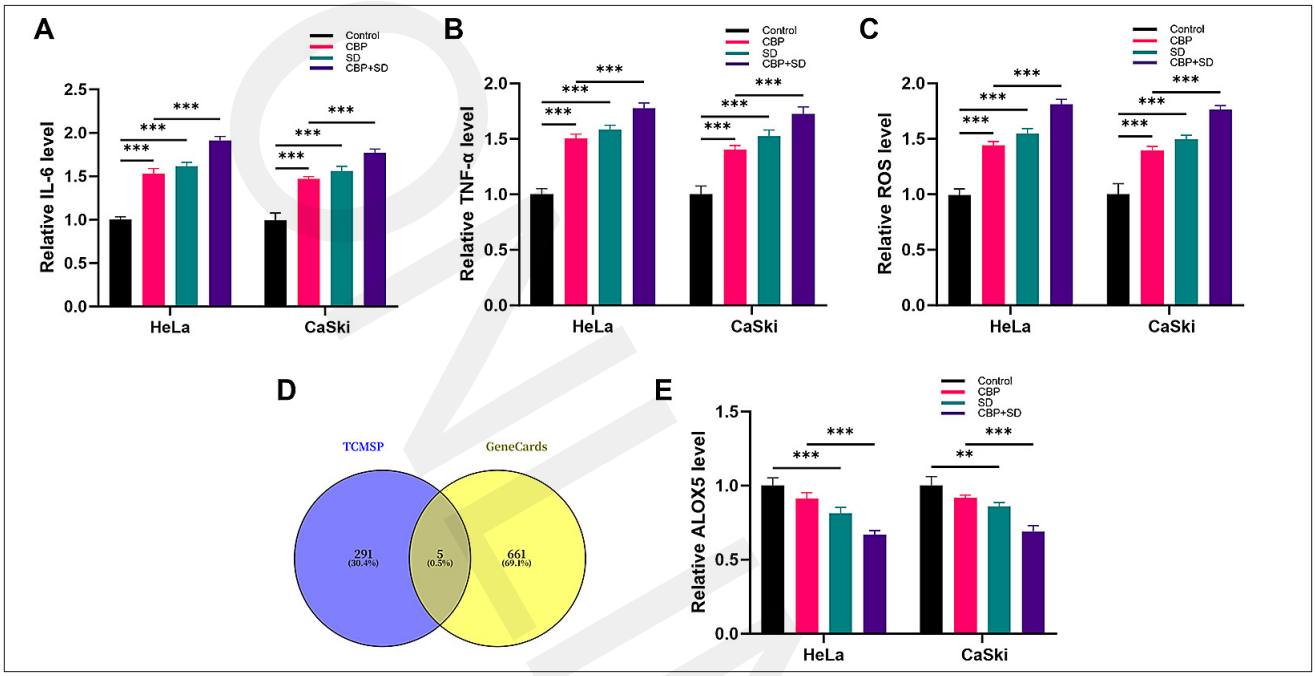



**Figure 4.** Mechanistic effects of SD combined with CBP in HeLa and CaSki cells. **(A)** IL-6 levels in HeLa and CaSki cells after SD-CBP combination treatment. (**B**) TNF-α levels in HeLa and CaSki cells after SD-CBP combination treatment. (**C**) Intracellular ROS levels in HeLa and CaSki cells after SD-CBP combination treatment. **(D)** Venn diagram of overlapping target genes between SD and cervical cancer. (**E**) ALOX5 mRNA expression in HeLa and CaSki cells after SD-CBP combination treatment. Data are shown as mean ± SD from 3 independent experiments (n=3).
$^{**}p < 0.01$; $^{***}p < 0.001$

efficiency was validated by RT-qPCR. As shown in Figure 5A, ALOX5 mRNA levels were reduced by approximately 51% in HeLa cells (from 2.45 to 1.19) and by approximately 52% in CaSki cells (from 2.41 to 1.16) following si-ALOX5 transfection, confirming successful knockdown. Functional assays revealed that knockdown of ALOX5 significantly reduced cell viability (Figure 5B-C), as well as migration and invasion capabilities (Figure 5D-E), in both HeLa and CaSki cells. Moreover, ALOX5 knockdown also led to increased levels of inflammatory cytokines (Fig. 5F-G) and elevated intracellular ROS (Fig. 5H). Taken together, these results suggested that down-regulation of ALOX5 not only inhibits proliferation, migration, and invasion of CC cells, but also enhances inflammatory response and oxidative stress, which may collectively contribute to the suppression of malignant progression.

## DISCUSSION

For locally advanced or early-stage CC, conventional treatments mainly include surgery, chemotherapy, and radiotherapy. Chemotherapy is commonly used for patients with advanced or recurrent disease, but its efficacy is often limited by the development of chemoresistance in cancer cells [26]. Notably, approximately 50% of patients experience recurrence or metastasis after treatment, with recurrence rates reaching to 50%–70% in stages IIB–IVA of the disease [17]. Therefore, the development of novel therapeutic strategies and agents is critical for improving clinical outcomes in CC.

TCM herbs are frequently employed as complementary or alternative approaches in cancer therapy due to their diverse chemical compositions, favourable safety profiles, and wide availability [2]. SD, a natural botanical extract, has been utilized in the treatment of various malignancies [27–29]. Studies have shown that SD inhibits the proliferation and migration of hepatocellular carcinoma cells without inducing significant weight loss or hepatorenal toxicity in animal models [30]. Furthermore, SD exhibits anti-inflammatory effects by targeting the STAT3 signalling pathway, and has been investigated for its potential application in lung cancer treatment [20].

SD exhibits physiological activity in various types of cancer. Its monomeric components have been shown to inhibit CC. However, the overall mechanism of action of the SD extract in CC remains poorly understood. Based on this background, the present study further investigated the effects of the ethanol extract of SD in HeLa and CaSki cell models. The results indicated that the extract influences several malignant biological behaviours of cells, specifically by inhibiting proliferation, migration, and invasion. The above findings suggested that the SD ethanol extract may intervene in the progression of CC through multiple targets and multiple pathways. Its effect may be attributed not only to a single known component, but also to the synergistic action of multiple components in the extract.

The present study further investigated the anti-CC effects of SD combined with CBP. Experimental results indicated that SD and CBP together exhibited synergistic effects *in vitro*. Compared to monotherapy, the combination treatment more significantly inhibited the proliferation, migration, and invasion of HeLa and CaSki cells, while also elevating IL-6, TNF-α, and intracellular ROS levels. The elevated levels of inflammatory cytokines and increased ROS observed suggest that the combination of SD and CBP triggers a pro-inflammatory cytotoxic stress response. This phenomenon, characterized by the acute and robust production of inflammatory mediators and ROS, is fundamentally distinct from chronic tumour-promoting inflammation. Studies have shown that TNF-α exerts direct cytotoxic effects on

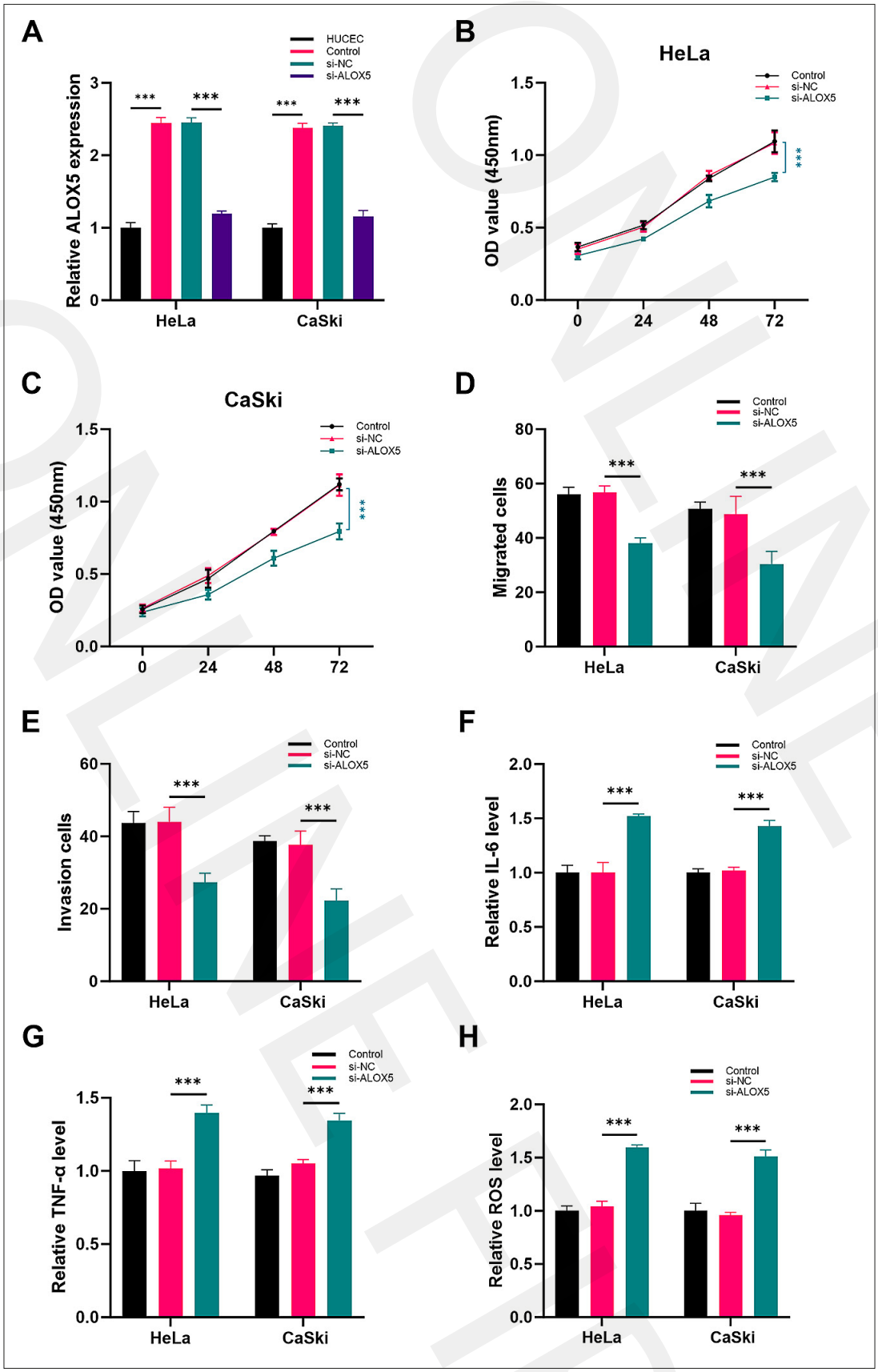



**Figure 5.** Effects of ALOX5 knockdown on biological behaviors of HeLa and CaSki cells. **(A)** ALOX5 mRNA expression levels in HeLa and CaSki cells after siRNA transfection. **(B)** Viability of HeLa cells after knockdown of ALOX5. **(C)** Viability of CaSki cells after knockdown of ALOX5. **(D)** Migration abilities of HeLa and CaSki cells following ALOX5 silencing. **(E)** Invasion abilities of HeLa and CaSki cells following ALOX5 silencing. **(F)** IL-6 levels in HeLa and CaSki cells after ALOX5 knockdown. **(G)** TNF-α levels in HeLa and CaSki cells after ALOX5 knockdown. **(H)** Intracellular ROS levels in HeLa and CaSki cells after ALOX5 knockdown. Data are presented as mean ± SD of 3 independent experiments (n=3).
$^{**}p < 0.01$; $^{***}p < 0.001$

cancer cells, especially under oxidative stress, supporting its potential as an anticancer agent [31, 32]. Furthermore, IL-6 can sensitize cancer cells to the extrinsic apoptotic pathway by upregulating death receptors (DR4 and DR5) in a p53-dependent manner, thereby enhancing TNF-α-induced and TRAIL-mediated cell death [33].

Previous studies have indicated that combining herbal medicines with Western drugs or other herbs holds promise for improving patient prognosis in various cancers. For instance, the combination of *Scutellaria barbata* D. Don (SB) and SD (SB-SD) is commonly used in the treatment of ovarian cancer [2]. In CC, the combination of paclitaxel, CBP, and bevacizumab has also been demonstrated to be effective and well-tolerated in patients with advanced or recurrent disease [34]. The findings of this study suggested that the combination of SD and CBP may substantially interfere with the malignant biological behaviours of CC cells, providing experimental support for potential clinical combination therapy. Mechanistically, combining herbal extracts with chemotherapeutic agents can enhance anti-tumour efficacy via multiple pathways, including regulating oxidative stress, inducing cell cycle arrest, inhibiting signalling pathways, or reversing drug resistance [35]. The observed synergistic increases in inflammatory cytokines, along with elevated ROS levels, suggested that activation of inflammatory pathways and oxidative damage may contribute to the mechanism of the combined treatment. These findings implied that SD and CBP may cooperatively modulate oxidative stress and inflammatory responses, thereby enhancing the inhibitory effect on CC cells.

This study also observed elevated ALOX5 expression in HeLa and CaSki cells, which was significantly down-regulated following combined treatment with SD and CBP. Previous studies have indicated that up-regulated ALOX5 expression is associated with disease progression across various tumours. In pancreatic cancer, ALOX5 has been shown to promote M2 macrophage polarization, enhance cancer cell invasion and metastasis, and correlate with poor clinical prognosis [36]. In addition, other studies have reported that ALOX5 and its metabolite 5-HETE are significantly up-regulated in CC compared with normal tissues, and ALOX5 inhibitors exhibit significant anti-cancer activity in this malignancy [18]. Consistent with these findings, in the current study, the loss-of-function experiments using siRNA-mediated ALOX5 knockdown revealed that silencing ALOX5 significantly inhibited the proliferation of both HeLa and CaSki cells, as demonstrated by reduced OD values in CCK-8 assays over 72 hours. Furthermore, transwell assays showed that ALOX5 knockdown markedly suppressed cell migration and invasion in both cell lines. In parallel, ALOX5 silencing not only suppressed the proliferation, migration, and invasion of CC cells but also triggered an acute cytotoxic stress response, as evidenced by elevated levels of pro-inflammatory cytokines (IL-6, TNF-α) and intracellular ROS. While chronic low-grade inflammation typically promotes tumourigenesis, the acute and robust release of these factors following ALOX5 inhibition represents a stress response that reflects lethal metabolic imbalance in cancer cells deprived of a survival shield, rather than the establishment of a tumour-promoting microenvironment.

These findings indicate that ALOX5 functions as a pro-survival factor critical for maintaining redox homeostasis and protecting CC cells from stress-induced death. Mechanistically, ALOX5 knockdown may disrupt arachidonic acid metabolism, leading to the accumulation of lipid mediators and activation of death pathways, possibly through modulating mitochondrial function [37]. Together, these results show that ALOX5 modulates key oncogenic processes in CC cells, and its disruption leads to ROS accumulation, inflammatory cytokine production, and the subsequent inhibition of malignant phenotypes. This evidence further supports the rationale for targeting ALOX5 in CC therapy.

**Limitations of the study.** This study also had several notable limitations. First, all experiments were performed only at the cellular level *in vitro*, and no *in vivo* studies using animal models were conducted to validate the anti-tumour effects of SD combined with CBP, which limits the translational significance of the findings. Second, the expression of ALOX5 was solely detected at the transcriptional level by RT-qPCR, and no further verification was performed at the protein level, such as Western blotting or immuno-fluorescence staining, weakening the reliability of the mechanistic conclusions. Third, the underlying molecular pathways were not fully confirmed; in particular, the involvement of ferroptosis and its representative markers was not explored, resulting in an incomplete interpretation of the mechanism underlying the synergistic effect. In addition, the synergistic mechanisms mediated by specific active components in SD with CBP were not elucidated in depth. Furthermore, the UPLC chromatographic fingerprint and detailed flavonoid composition of the SD extract were not provided, which somewhat compromises the reproducibility of the experiments.

Future studies should focus on *in vivo* validation in appropriate animal models, protein-level detection of ALOX5, identification of ferroptosis and other related signalling pathways, as well as the pharmacokinetic and pharmacodynamic interactions of key components in SD combined with CBP, and comprehensive chemical characterization of the extract.

## CONCLUSIONS

In summary, the combination of SD and CBP significantly suppressed proliferation, migration, and invasion, while elevating IL-6, TNF-α, and intracellular ROS levels in HeLa and CaSki cells. Modulation of ALOX5 expression was further shown to inhibit malignant behaviours in these cancer cells.

### Acknowledgements
This study was funded by Fujian Provincial Health Commission Science and Education Division Youth Research Project, 2024QNA067; NATCM'Project of High-level Construction of Key TCM Disciplines(Clinical Integration of Traditional Chinese and Western Medicine), zyyzdxk-2023104.

## REFERENCES

1. He ZY, Li HY, Yan J, et al. A prospective trial to evaluate the clinical efficacy and safety of neoadjuvant chemotherapy with arsenic trioxide

and carboplatin in locally advanced cervical cancer: a study protocol for randomized controlled clinical. Trials. 2022;23(1):556. https://doi.org/10.1186/s13063-022-06489-1
2. Wang Z, Liu M, Li GX, et al. A herbal pair of Scutellaria barbata D. Don and Scleromitrion diffusum (Willd.) R.J. Wang induced ferroptosis in ovarian cancer A2780 cells via inducing heme catabolism and ferritinophagy. J Integr Med. 2024;22(6):665–82. https://doi.org/10.1016/j.joim.2024.10.001
3. Yang PW, Chen TT, Zhao WX, et al. Scutellaria barbata D. Don and Oldenlandia diffusa (Willd.) Roxb crude extracts inhibit hepatitis-B-virus-associated hepatocellular carcinoma growth through regulating circRNA expression. J Ethnopharmacol. 2021;275:114110. https://doi.org/ 10.1016/j.jep.2021.114110
4. Kedhari Sundaram M, Raina R, Afroze N, et al. Quercetin modulates signaling pathways and induces apoptosis in cervical cancer cells. Biosci Rep. 2019;39(8). https://doi.org/ 10.1042/BSR20190720
5. He C, Lu X, Li J, et al. The effect of quercetin on cervical cancer cells as determined by inducing tumor endoplasmic reticulum stress and apoptosis and its mechanism of action. Am J Transl Res. 2021;13(5):5240–7.
6. Chen X, Xu P, Zhang H, et al. EGFR and ERK activation resists flavonoid quercetin-induced anticancer activities in human cervical cancer cells in vitro. Oncol Lett. 2021;22(5):754. https://doi.org/10.3892/ol.2021.13015.
7. Ji H, Li K, Xu W, et al. Prediction of the Mechanisms by Which Quercetin Enhances Cisplatin Action in Cervical Cancer: A Network Pharmacology Study and Experimental Validation. Front Oncol. 2021;11:780387. https://doi.org/10.3389/fonc.2021.780387.
8. Choi EY, Han EJ, Jeon SJ, et al. Kaempferol Inhibits Cervical Cancer Cells by Inducing Apoptosis and Autophagy via Inactivation of the PI3K/AKT/mTOR Signaling Pathway. Anticancer Res. 2024;44(7):2961–72. https://doi.org/10.21873/anticanres.17108
9. Liu Q, Chen X, Tan Y, et al. Natural products as glycolytic inhibitors for cervical cancer treatment: A comprehensive review. Biomed Pharmacother. 2024;175:116708. https://doi.org/10.1016/j.biopha.2024.116708
10. Chen Y, Yu D, Zhu D, et al. Exploring alkaloids and flavonoids from natural sources: Emerging natural agents for inhibiting cervical cancer progression through apoptosis induction, anti-inflammatory effects, and oxidative stress reduction. Pathol Res Pract. 2025;272:156092. https://doi.org/10.1016/j.prp.2025.156092
11. Tu LY, Bai HH, Cai JY, Deng SP. The mechanism of kaempferol induced apoptosis and inhibited proliferation in human cervical cancer SiHa cell: From macro to nano. Scanning. 2016;38(6):644–53. https://doi.org/10.1002/sca.21312
12. Guan F, Du H, Li J, et al. Quercetin Alleviates LPS-Stimulated Myocardial Injury through Regulating ALOX5/PI3K/AKT Pathway in Sepsis. Cardiovasc Toxicol. 2024;24(10):1116–24. https://doi.org/10.1007/s12012-024-09901-1
13. Yoshimoto T, Furukawa M, Yamamoto S, et al. Flavonoids: potent inhibitors of arachidonate 5-lipoxygenase. Biochem Biophys Res Commun. 1983;116(2):612–8. https://doi.org/10.1016/0006-291x(83)90568-5
14. Marin L, Gutierrez-Del-Rio I, Entrialgo-Cadierno R, et al. De novo biosynthesis of myricetin, kaempferol and quercetin in Streptomyces albus and Streptomyces coelicolor. PLoS One. 2018;13(11):e0207278. https://doi.org/10.1371/journal.pone.0207278
15. Zargar S, Altwaijry N, Wani TA, Alkahtani HM. Evaluation of the Possible Pathways Involved in the Protective Effects of Quercetin, Naringenin, and Rutin at the Gene, Protein and miRNA Levels Using In-Silico Multidimensional Data Analysis. Molecules. 2023;28(13). https://doi.org/10.3390/molecules28134904
16. Liu T, Xu X, Li J, et al. ALOX5 deficiency contributes to bladder cancer progression by mediating ferroptosis escape. Cell Death Dis. 2023;14(12):800. https://doi.org/10.1038/s41419-023-06333-7
17. Zhao F, Hong J, Zhou G, et al. Elucidating the role of tumor-associated ALOX5+ mast cells with transformative function in cervical cancer progression via single-cell RNA sequencing. Front Immunol. 2024;15:1434450. https://doi.org/10.3389/fimmu.2024.1434450
18. Li L, Xiao Y, Xu Z, Wang S. Zileuton inhibits arachidonate-5-lipoxygenase to exert antitumor effects in preclinical cervical cancer models. Cancer Chemother Pharmacol. 2021;88(6):953–60. https://doi.org/10.1007/s00280-021-04343-w
19. Shan K, Feng N, Zhu D, et al. Free docosahexaenoic acid promotes ferroptotic cell death via lipoxygenase dependent and independent pathways in cancer cells. Eur J Nutr. 2022;61(8):4059–75. https://doi.org/10.1007/s00394-022-02940-w
20. Ye W, Zhao Q, Li P, Zhou T. Scleromitrion diffusum (Willd.) R. J. Wang Inhibits Gastric Cancer via ERBB2/ERBB3/PI3K/AKT Pathway. Turk J Gastroenterol. 2024;35(11):831–8. https://doi.org/10.5152/tjg.2024.24152
21. Banerjee V, Sharda N, Huse J, et al. Synergistic potential of dual andrographolide and melatonin targeting of metastatic colon cancer cells: Using the Chou-Talalay combination index method. Eur J Pharmacol. 2021;897:173919. https://doi.org/10.1016/j.ejphar.2021.173919
22. Saha S, Sultana S, Rahmat R, et al. Patterns of Different Cervical Cytokine Expression in High-Risk Human Papillomavirus-Infected Patients With Cervical Cancer and Its Precancerous Lesions. Clin Med Insights Oncol. 2025;19:11795549251316767. https://doi.org/10.1177/11795549251316767
23. Li Q, Kaidong L, Tian Z, et al. Association of Inflammatory Factors with Cervical Cancer: A Bidirectional Mendelian Randomization. J Inflamm Res. 2024;17:10119–30. https://doi.org/10.2147/JIR.S493854
24. Tomaziu-Todosia Anton E, Anton GI, Scripcariu IS, et al. Oxidative Stress, Inflammation, and Antioxidant Strategies in Cervical Cancer-A Narrative Review. Int J Mol Sci. 2025;26(10). https://doi.org/10.3390/ijms26104961
25. Wang L, Wang B. ALOX5 regulates vascular smooth muscle cells pyroptosis to affect abdominal aortic aneurysm formation. Sci Rep. 2025;15(1):29123. https://doi.org/10.1038/s41598-025-14268-6
26. Zhou J, Guo Z, Peng X, et al. Chrysotoxine regulates ferroptosis and the PI3K/AKT/mTOR pathway to prevent cervical cancer. J Ethnopharmacol. 2025;338(Pt 3):119126. https://doi.org/10.1016/j.jep.2024.119126
27. Feng J, Jin Y, Peng J, et al. Hedyotis diffusa willd extract suppresses colorectal cancer growth through multiple cellular pathways. Oncol Lett. 2017;14(6):8197–205. https://doi.org/10.3892/ol.2017.7244
28. Song Y, Wang H, Pan Y, Liu T. Investigating the Multi-Target Pharmacological Mechanism of Hedyotis diffusa Willd Acting on Prostate Cancer: A Network Pharmacology Approach. Biomolecules. 2019;9(10). https://doi.org/10.3390/biom9100591
29. Yeh YC, Chen HY, Yang SH, et al. Hedyotis diffusa Combined with Scutellaria barbata Are the Core Treatment of Chinese Herbal Medicine Used for Breast Cancer Patients: A Population-Based Study. Evid Based Complement Alternat Med. 2014;2014:202378. https://doi.org/10.1155/2014/202378
30. Huang L, Xu H, Wu T, Li G. Hedyotis diffusa Willd. Suppresses Hepatocellular Carcinoma via Downregulating AKT/mTOR Pathways. Evid Based Complement Alternat Med. 2021;2021:5210152. https://doi.org/10.1155/2021/5210152
31. Yang L, Wang Y, Shi S, et al. The TNF-alpha-induced expression of miR-130b protects cervical cancer cells from the cytotoxicity of TNF-alpha. FEBS Open Bio. 2018;8(4):614–27. https://doi.org/10.1002/2211-5463.12395
32. Valenzuela Cardenas M, Nowicki TS. TNF-alpha: Roles in pathogenesis and therapeutics in cancer. J Biol Chem. 2026;302(3):111251. https://doi.org/10.1016/j.jbc.2026.111251
33. Sano E, Kazaana A, Tadakuma H, et al. Interleukin-6 sensitizes TNF-alpha and TRAIL/Apo2L dependent cell death through upregulation of death receptors in human cancer cells. Biochim Biophys Acta Mol Cell Res. 2021;1868(7):119037. https://doi.org/10.1016/j.bbamcr.2021.119037
34. Suzuki K, Nagao S, Shibutani T, et al. Phase II trial of paclitaxel, carboplatin, and bevacizumab for advanced or recurrent cervical cancer. Gynecol Oncol. 2019;154(3):554–7. https://doi.org/10.1016/j.ygyno.2019.05.018
35. Huang W, Wen F, Yang P, et al. Yi-qi-hua-yu-jie-du decoction induces ferroptosis in cisplatin-resistant gastric cancer via the AKT/GSK3beta/NRF2/GPX4 axis. Phytomedicine. 2024;123:155220. https://doi.org/10.1016/j.phymed.2023.155220
36. Hu WM, Liu SQ, Zhu KF, et al. The ALOX5 inhibitor Zileuton regulates tumor-associated macrophage M2 polarization by JAK/STAT and inhibits pancreatic cancer invasion and metastasis. Int Immunopharmacol. 2023;121:110505. https://doi.org/10.1016/j.intimp.2023.110505
37. Amoah AS, Pestov NB, Korneenko TV, et al. Lipoxygenases at the Intersection of Infection and Carcinogenesis. Int J Mol Sci. 2024;25(7). https://doi.org/10.3390/ijms25073961